JOURNAL OF MATERIALS SCIENCE 13 (1978) 367–376

Microstructural changes which occur during isochronal heat treatment of the nickel-base superalloy IN-738

R. A STEVEN, P. E. J. FLEWITT
Central Electricity Generating Board, South Region Scientific Services Department, West Farm Place, Chalk Lane, Cockfosters, Barnet, Herts., UK

The microstructure of the cast superalloy IN-738 has been analysed after isochronal heat treatments (16 h) within the temperature range 773 to 1467 K. The effect of such heat treatments on the morphology, distribution and volume fraction of both γ' and carbide precipitates has been established and correlated with changes in the hardness. These measured hardness changes are discussed in relation to the contributions of γ' precipitation hardening and matrix solid solution hardening.

1. Introduction

The nickel-base superalloy IN-738 is being introduced as a blade material in the high pressure (HP) stage of land-based gas turbines, due to its superior high temperature mechanical properties and improved corrosion resistance when compared with the existing Nimonic 105/115 alloys [1]. Such gas turbine units are used within the Central Electricity Generating Board since they provide a flexible means of generating electricity [2].

The cast microstructure of IN-738 comprises a uniform dispersion of small ordered γ' precipitates, together with carbide particles, both of which are distributed within a face-centred cubic (f c c) γ matrix [3]. As with most commercial cast and wrought nickel-base superalloys the mechanical strength and creep resistance depend upon three main contributions [4]:

(a) Solid solution strengthening of the disordered γ f c c matrix which is achieved by the additions of elements such as aluminium, chromium molybdenum, tungsten and cobalt.

(b) The presence of coherent precipitates of γ' phase which has an ordered f c c structure, $L1_2$, based on the Ni_3 (Al, Ti) composition. In general γ' precipitates as regular or degenerate cuboids of mean diagonal 0.5 μm, or spheroids of approximately 0.1 μm diameter. Hagel and Beattie [5] observed that the morphology is governed by lattice mismatch such that spheres occur at 0 to 0.2% mismatch, which become cubes at 0.5 to 1% mismatch and then become plates if the mismatch exceeds ~ 1.3%.

(c) Grain-boundary strengthening by metallic carbides and borides.

In this paper the effect of isochronal heat treatment on the morphology, distribution and volume fraction of both γ' and carbide precipitates has been examined and correlated with changes in hardness.

2. Experimental procedure

An alloy of IN-738 was prepared by vacuum induction melting of high purity materials to produce an ingot of approximately 110 mm diameter and 250 mm length. The chemical analysis for this ingot is given in Table I. The standard recommended heat treatment for IN-738 blades involves a partial solution treatment for 2 h at 1393 K, followed by ageing for 16 h or 24 h at 1118 K, cooling in air after each stage. Specimens of approximately 10 mm × 10 mm × 3 mm were machined from the ingot. To produce a uniform initial microstructure, all specimens were subjected to the partial solution treatment followed by rapid quenching into iced brine; such quenching has been shown to provide a sufficiently fast cooling rate [6] which would suppress further precipitation of γ'. Isochronal heat treatment on a series

of these specimens was carried out for 16 h at temperatures within the range 773 K to 1467 K. A further series of specimens was used to investigate precipitate development for times up to ~610 h at 973 K, whilst other heat treatments were carried out to establish the γ' solvus temperature. Again, specimens were quenched into iced brine after heat treatment, to retain the microstructures developed at the respective temperatures.

The weight fractions of γ' and carbides were established using the electrolytic extraction technique described by Kriege and Baris [7]. Anodic dissolution of the matrix was carried out at 293 K in an electrolyte containing 10 g ammonium sulphate and 10 g citric acid in 1000 ml water at 4 V. The residue, which comprised the total precipitate content, was allowed to settle and was then separated, dried and weighed to establish the weight fraction. Since carbides and borides are insoluble in this electrolyte a different method was used to determine their contribution to the total weight fraction of precipitate. Here anodic dissolution was carried out at 8 V in an electrolyte containing 100 ml hydrochloric acid, 10 g tartaric acid, and 900 ml methyl alcohol [7]. This results in the dissolution of both γ matrix and the γ' precipitates, thereby allowing the carbide and boride weight fraction to be measured. The weight fraction of γ' precipitate was therefore established by difference; this was then approximated to the volume fraction [8].

For optical metallography, specimens were polished and etched in a reagent containing 7.5 g ferric chloride, 7.5 g cupric chloride, 150 ml water, 300 ml hydrochloric acid and 50 ml nitric acid. For more detailed observation of this microstructure carbon replicas shadowed with a gold–palladium alloy were taken from the specimen surfaces. Thin foils were prepared by spark-machining 3 mm diameter discs from the bulk specimens. These discs were profiled and thinned using electrochemical jetting at 20 V in an electrolyte containing 5% perchloric acid in ethanol maintained at ~263 K. After perforation the foils were finally polished for 5 sec with the same electro-polishing conditions, but using a modified PTFE holder technique [9]. This latter procedure facilitated rapid washing of the foils in ethanol and ensured clean foils were produced. Both foils and replicas were examined at 100 kV in an AEI EM 802 transmission electron microscope (TEM) equipped with a double tilt stage.

The sizes of the larger cuboidal γ' particles were measured directly from photographs of carbon replicas using a Zeiss (TGZ3) size analyser. To enable an adequate distribution to be obtained, approximately 500 particles per sample were measured. This gave reproducible results and eliminated variations due to microstructural inhomogeneities. The iris diameter was adjusted to produce an equivalent area to that of the particle measured, so that optical determinations of the area fraction could be converted to volume fraction of γ' and compared with the values obtained by electrolytic extraction. These measurements show the change in average particle size with ageing temperature, but do not give an absolute size for a given ageing temperature since the indeterminate particle morphology complicates the necessary sectioning corrections described by Underwood [10]. For size measurements of the small spheroidal γ' particles, a suspension of electrolytically extracted residue in acetone was ultrasonically agitated to prevent particle agglomeration and allowed to dry on a carbon support film which had been evaporated onto a 100 mesh copper electron microscope grid. This was recoated with carbon and, when examined in the TEM, individual particles could be resolved and measured. The method has the advantage that geometrical corrections are not required for spherical particles.

X-ray analysis of extracted carbide particles was carried out using a Philips powder camera of 114.6 mm diameter with a Straumanis film mounting and Cu$K\alpha$ radiation ($\lambda = 0.1542$ nm).

3. Results

3.1. 'As-cast' microstructure

The microstructure of IN-738 in the 'as-cast' condition is shown in Fig. 1a. Essentially this comprises irregularly shaped grains of γ phase, whose boundaries are, in part, defined by concentrations of carbide particles and other precipitates. Within the grains, more carbide particles and small micropores (~10 μm) are visible. There is also evidence of 'coring' (dendritic segregation), where the darker etched areas contain higher concentrations of γ' precipitates. Observations of carbon replicas in the TEM (Fig. 1b) reveal a large variation in γ' precipitate size and morphology,

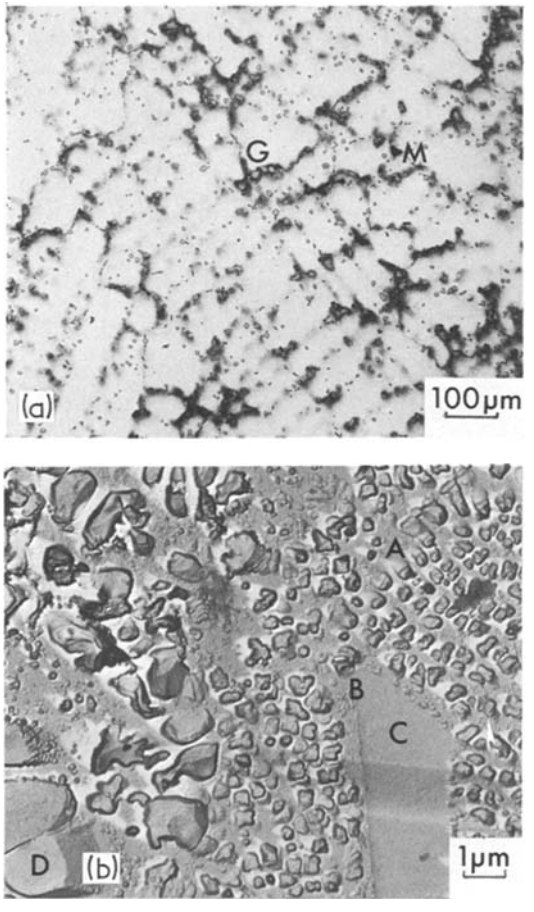

Figure 1 'As-cast' microstructure of IN-738: (a) optical micrograph showing the cored dendritic structure. Grain boundaries are partially delineated by carbide and γ' precipitates, as at G, and micropores are visible, as at M. $FeCl_3/CuCl_2/HCl/HNO_3$ etchant; (b) carbon/gold-palladium replica showing precipitates of (i) γ' cuboids, at A, (ii) γ' spheroids, at B, (iii) carbides, at C. (iv) eutectic ($\gamma + \gamma'$) product, at D.

from cuboids of mean diagonal $\sim 0.4\,\mu m$ to spheroids of diameter $\sim 0.05\,\mu m$. At D, sections of coarse γ' rods, which form possibly by eutectic decomposition, are present. The observed microstructure is typical of that described for this alloy by Bieber and Mihalisin [3].

3.2. Solvus temperature for γ'

To determine the solvus temperature (the upper limit for precipitation of the γ' phase), thermocouples were secured directly to the specimens for precise temperature control. The specimens were only aged for one hour before quenching since the kinetics of γ' dissolution are rapid as the solvus temperature is approached [8]. An initial series of specimens aged at 10 deg intervals within the range 1373 to 1473 K located the solvus temperature between 1433 and 1453 K, as indicated by the presence or absence of γ' particles on optical micrographs. Further heat treatments within this temperature range established the solvus temperature as 1442 ± 3 K.

3.3. Isochronal heat treatment

3.3.1. Hardness

The variation of room temperature Vickers hardness, Hv_{30}, with isochronal ageing temperature is shown in Fig. 2a. After ageing at 773 K, the hardness is unchanged from the value which results from solution treatment only. However, as the ageing temperature increases, the hardness rises to a maximum ($Hv \approx 485$) at ~ 1100 K, dropping to a minimum ($Hv \approx 325$) at ~ 1315 K, then rising again to $Hv \approx 440$ at ~ 1467 K.

3.3.2. Carbides and borides

The procedure described in Section 2 was used quantitatively to extract carbides and any borides present in the isochronally heat-treated specimens. Fig. 2b shows that above ~ 1425 K the weight fraction of carbides or borides decreases from a steady value of ~ 0.015, but even at 1473 K some

TABLE I Composition of the IN-738 ingot

Element	Analysis (wt %)
Carbon	0.17
Aluminium	3.53
Titanium	3.60
Aluminium + Titanium	7.13
Boron	0.012
Cobalt	8.40
Chromium	15.75
Molybdenum	1.69
Niobium	0.87
Tantalum	1.77
Tungsten	2.78
Zirconium	0.12
Nickel	Balance
Maximum impurity levels:	
Silicon	0.03
Manganese	0.03
Iron	0.07
Sulphur	–
Lead	–
Bismuth	–
Silver	–

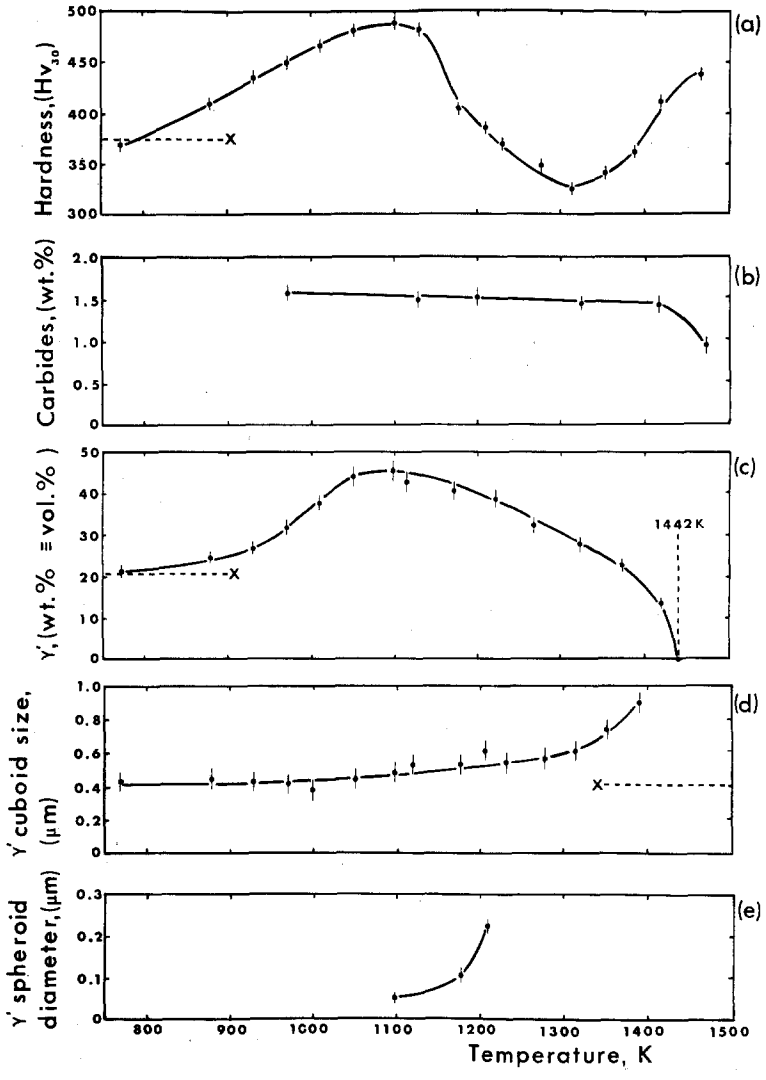

Figure 2 Variation with isochronal (16 h) ageing temperature of: (a) hardness, (b) carbide precipitate fraction, (c) total γ' precipitate fraction, (d) relative γ' cuboid size, as measured with Zeiss particle-size analyser (iris diameter which gives equivalent area to particle section), (e) γ' spheroid diameter X defines the values obtained after the solution treatment (2 h at 1393 K).

carbides remain, whereas all the γ' is in solution. X-ray analysis of the extracted residues shows only a f c c structure of mean lattice parameter 0.432 nm to be present. This structure and value for the lattice parameter is consistent with an MC-type carbide [11], which agrees with the observations of Decker and Sims [12], who show that very little $M_{23}C_6$ carbide forms. Small additions of boron, together with zirconium, are added to IN-738 to enhance creep properties by reducing the onset of grain boundary tearing [13]. In general, boron segregates to the grain boundaries, and Boesch and Canada [14] show that only when the boron content exceeds 120 p.p.m. does it react to form boride precipitates. The concentration of boron in the present alloy, ~ 120 p.p.m. (Table I), together with the non-detectability of borides by X-ray diffraction, is consistent with such a criterion.

3.3.3. γ' precipitation

Fig. 2c shows the weight fraction (≡ volume fraction) of electrolytically extracted γ', after correction for the carbide content, as a function of isochronal ageing temperature. Here error bars are based on electrolytic extraction from ten samples aged at the same temperature (1373 K). A maximum fraction of ~ 0.45 results from ageing at ~ 1100 K, which coincides with the maximum hardness (Fig. 2a). The fraction of γ' decreases steadily up to the solvus temperature, 1442 K, and there is also a decrease for ageing temperatures below 1100 K, such that at 773 K the fraction (0.215) is similar to that in a solution treated specimen. When examined in the TEM, carbon replicas taken from etched samples show several trends in γ' precipitation as the ageing temperature is increased. The solution treatment, 2 h at 1393 K, homogenizes the cast microstructure, producing a

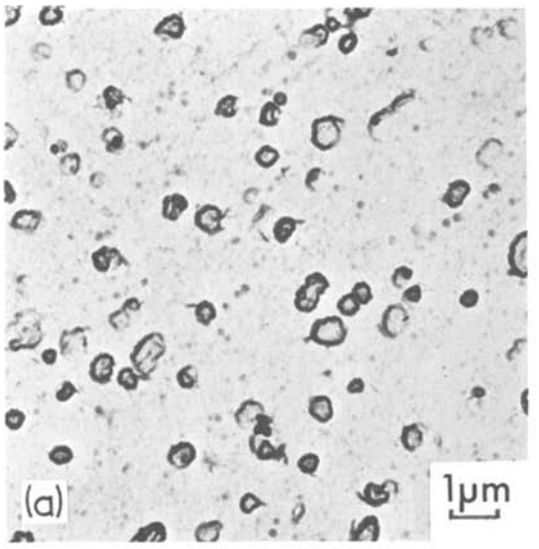

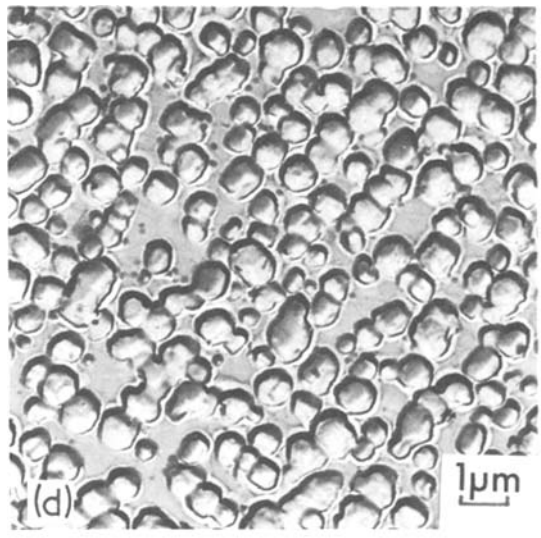

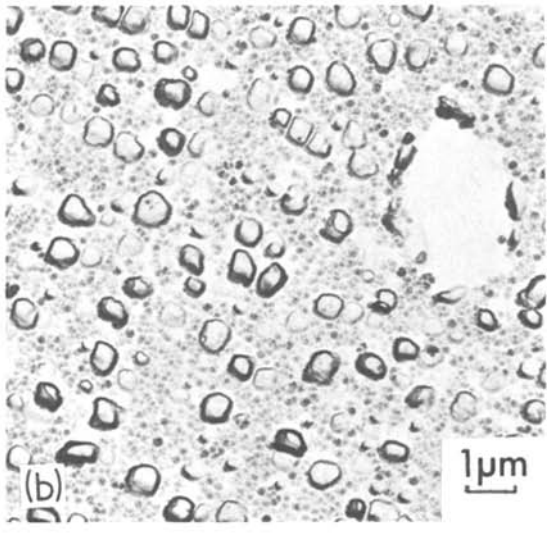

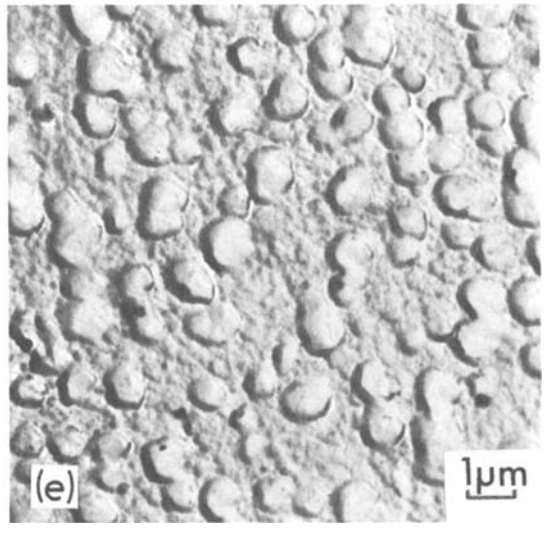

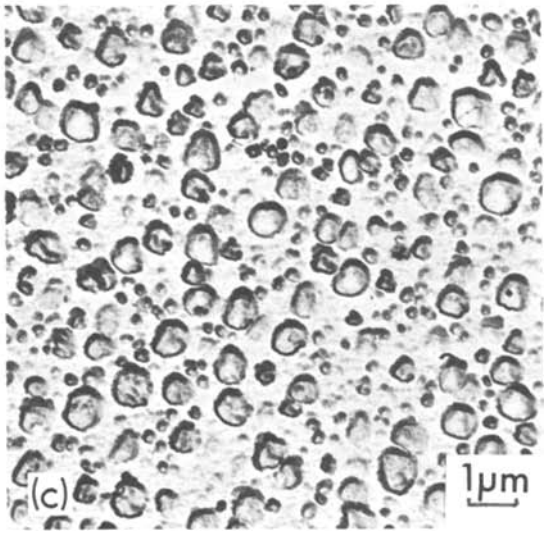

Figure 3 Carbon/gold-palladium replicas on IN-738 showing γ' precipitation after various isochronal (16 h) heat treatments; (a) 973 K. γ' spheroids beginning to develop, (b) 1100 K. γ' spheroids predominate, (c) 1177 K. γ' spheroids coarsening rapidly, (d) 1278 K. γ' spheroids disappeared; γ' cuboids coarsening, (e) 1393 K. Rapid coarsening and partial dissolution of γ' cuboids.

regular array of cuboidal γ' particles of uniform size ($\sim 0.4\,\mu$m). Such a microstructure persists after ageing at temperatures between 773 K and 930 K, but above 973 K small spheroidal γ' particles precipitate between the primary cuboids (Fig. 3a). At the temperature that corresponds to the maximum hardness and volume fraction (1100 K), numerous γ' spheroidal precipitation has occurred (Fig. 3b). At higher temperatures the spheroids continue to coarsen but become less

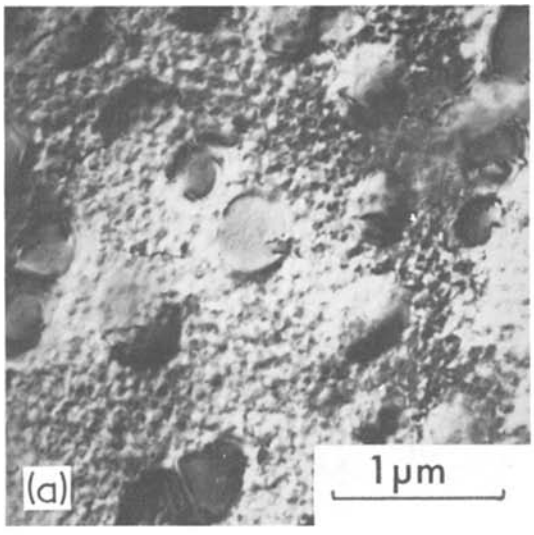

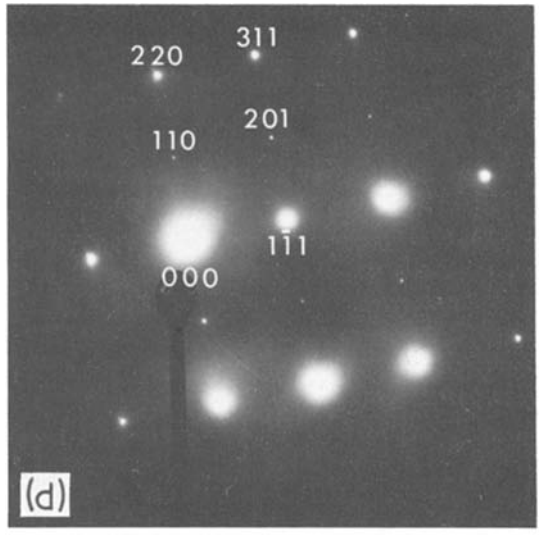

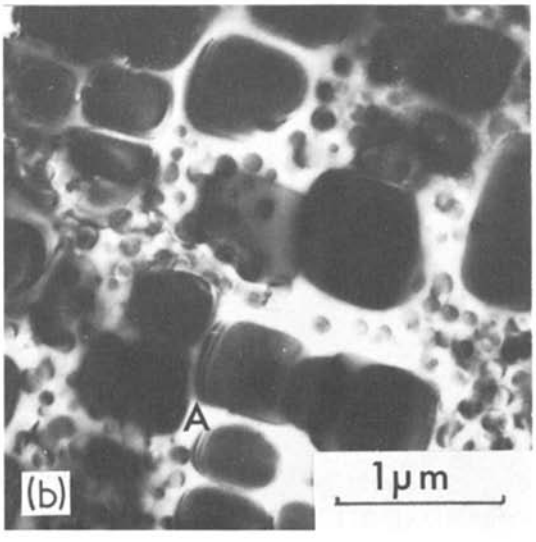

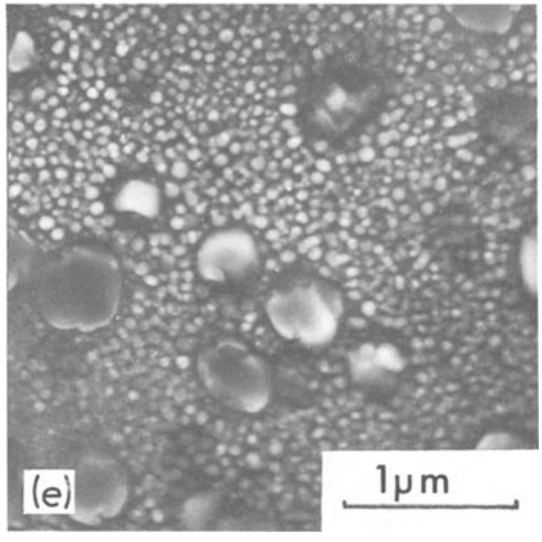

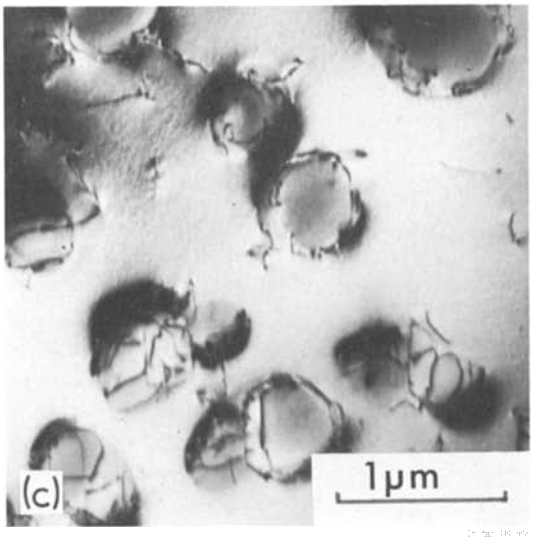

Figure 4 Transmission electron micrographs of thin foils of IN-738 subjected to various isochronal (16 h) heat treatments: (a) 1100 K, showing high density of γ' spheroids between γ' cuboids. Overlapping strain field contrast prevents resolution of individual spheroids, (b) 1177 K. Coarse γ' cuboids show δ -fringe contrast at A. A small fraction of γ' spheroids is visible between the cuboids, (c) 1393 K. Coarse γ' cuboids showing accommodation interfacial dislocations. No evidence of γ' spheroids in γ matrix, (d) Selected area diffraction pattern of γ' cuboid in (a), showing superlattice reflections. [1 1 2] zone axis, (e) 1100 K. High resolution dark field image taken using a superlattice reflection, showing that coarse γ' cuboids and fine γ' spheroids have the same crystal structure.

numerous (Fig. 3c), until at 1278 K (Fig. 3d) only cuboids remain. Figs. 2d and e show the sizes of cuboids and spheroids respectively for various ageing temperatures the cuboids also coarsen monotonically up to ~1315 K, above which the coarsening rate increases.

Thin foils were taken from the isochronally aged specimens and were examined in the TEM (Figs. 4a to e). Figs. 4a to c show the bright field images of the typical two sizes of γ' precipitate which develop at three heat treatment temperatures. The selected area electron diffraction pattern (Fig. 4d) contains a systematic array of superlattice reflections which satisfies a condition for h, k, l to be mixed [15]; however, because of their structure factor they are considerably weaker than the fundamental reflections. Careful inspection of this and similar patterns confirms that these reflections are derived from the ordered γ' structure ($L1_2$) and the absence of any reflections from a structure of tetragonal symmetry indicates that γ'' (DO_{22}) precipitates have not formed [16]. When the volume fraction of spheroidal γ' precipitates is large (Fig. 4a), individual spheroids cannot be resolved because of overlapping strain field contrast. However, high resolution centred dark field images obtained using a $L1_2$ superlattice reflection, Fig. 4e, confirm that the spheroids have the same crystal structure as the γ' cuboids. After ageing at 1393 K no γ' spheroids were observed, although several foils were examined, Fig. 4c. Furthermore, no extra reflections or side-bands to main reflections were observed in selected area diffraction patterns, thus confirming the absence of γ' spheroids above 1315 K. Throughout we have described the shape of the coarse γ' precipitates as cuboids; however, although in Fig. 4b rectangular cross-sections indicate a cubic geometry, foils examined with other [*hkl*] normals reveal sections of precipitate with a less regular shape. As a consequence these precipitates should be more correctly described as degenerate cuboids.

Precipitate contrast theory for superalloys has been discussed by Oblak and Kear [15]. Essentially for γ' precipitates the contrast arises from coherency strain, δ-fringe, displacement fringe and structure factor, although this can be enhanced by preferential thinning of the precipitates during electro-polishing. In Fig. 4b the γ' precipitates show δ-fringe contrast across the γ'/γ interfaces, typically at A. This contrast is the result of tetragonal distortion of the γ matrix immediate to the interface due to differences in lattice parameter. With selected values of the diffraction vector, **g**, the measured fringe spacing indicates the mismatch to be ~0.3% [15, 17]. This is of the order of the mismatch proposed by Hagel and Beattie [5] for γ' cuboids. However, at higher temperatures these precipitates become coarser and lose coherency as shown by the presence of accommodation interfacial dislocations after ageing at 1393 K (Fig. 4c) [18].

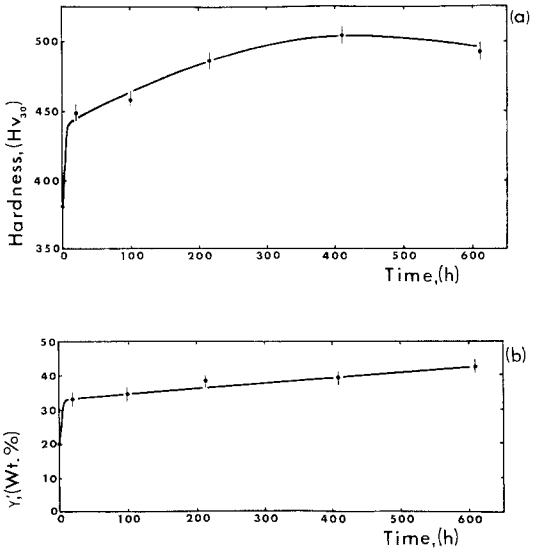

Figure 5 Variation of: (a) hardness after isothermal heat treatment of IN-738 at 973 K, (b) γ' fraction with time, after isothermal heat treatment of IN-738 at 973 K.

3.4. Long-term ageing

Isothermal heat treatments were carried out to investigate the decrease in both hardness and γ' fraction for isochronal ageing below the optimum temperature (1100 K). Fig. 5 shows that after the recommended solution treatment (2 h at 1393 K), the alloy has a γ' fraction of 0.2 and a hardness of $Hv = 381$. Subsequent ageing for 16 h at 973 K increases the γ' fraction to 0.32 and the hardness to $Hv = 450$. Further ageing for times up to ~610 h at 973 K increases the γ' fraction to 0.42 and the hardness to $Hv = 492$, which are comparable to the values obtained from samples aged for 16 h to peak hardness, Figs. 2a and c. The decrease in hardness for isochronal ageing below 1100 K is therefore simply explained by incomplete precipitation of γ' spheroids in the 16 h period.

4. Discussion

The heat treatment which is recommended for the cast superalloy IN-738 was based on the comparison of yield strengths after a series of heat treatments [3]. However, there was little attempt to carry out these heat treatments systematically or even to determine the solvus temperature for γ' precipitation. The present results establish the solvus temperature as 1442 K so that the recommended solution treatment of 2 h at 1393 K results in only partial dissolution of the γ' (Fig. 2c), and in fact the volume fraction remaining at this temperature is ~ 0.2. The recommended heat treatment involves air cooling rather than quenching after each stage, but nevertheless it is reasonable to assume that the ageing treatment (16 h at 1118 K) will produce near-maximum hardness, Fig. 2a.

The maximum hardness ($Hv = 485$) and the minimum hardness ($Hv = 325$) are achieved by isochronal ageing at 1100 K and 1315 K (Fig. 2a), at which temperatures the volume fractions of γ' precipitates are 0.45 and 0.3 respectively, Fig. 2c. However, representative counts from replicas show the corresponding γ' cuboid densities to be $1.143 \times 10^6\ \mathrm{mm}^{-2}$ and $1.070 \times 10^6\ \mathrm{mm}^{-2}$. This small discrepancy is probably due to linking of particles at the higher temperature. These data, together with the particle sizes shown in Fig. 2d, give the volume fractions for the γ' cuboids as 0.214 (1100 K) and 0.307 (1315 K). At 1315 K all the precipitates are degenerate cuboids; consequently there is good agreement between the electrolytic and optical determination of volume fraction without the requirement for the geometrical corrections proposed by Underwood [10]. Furthermore, at 1100 K the small spheroidal γ' precipitates must account for the difference between the total measured fraction of 0.45 and that of the γ' cuboids (0.214), to give 0.236 of the total.

Stoloff [19] and Decker [13] have reviewed the mechanisms which contribute to the overall strength of the nickel-base superalloys. For precipitation hardened superalloys the Orowan bowing mechanism [20, 21] for γ' spheroids is generally considered to provide the largest contribution to the strength. The increment in the flow stress at low temperature is given by consideration of the radius of curvature to which the dislocation line can be bent between precipitate particles of radius r and separation L by the applied stress. This leads to an approximate expression for the increment in the flow stress [21]:

$$\Delta\tau = \frac{G\mathbf{b}}{2\pi L}\,\phi \ln \frac{L}{2\mathbf{b}} \qquad (1)$$

where G is the shear modulus ($7.4 \times 10^{10}\ \mathrm{Nm}^{-2}$), $\mathbf{b}$ is the Burger's vector (0.254 nm) and

$$\phi = \tfrac{1}{2}\left[1 + (1-\nu)^{-1}\right] \qquad (2)$$

where ν is Poisson's ratio (~ 0.3). The edge-to-edge spacing of particles is given by the relationship [22]:

$$L = 0.82r\left[\left(\frac{\pi}{F}\right)^{1/2} - 2\right] \qquad (3)$$

where F is the precipitate fraction.

After the heat treatment at 1100 K, the values of $F = 0.236$, $r = 0.0305\ \mu\mathrm{m}$, give an increment in flow stress due to the γ' spheroids of $\Delta\tau \approx 400\ \mathrm{MNm}^{-2}$. Individual linear conversions of hardness to yield or flow stress are valid for particular materials in particular strength ranges [23]. On this basis, the yield stress (σ_y) of IN-738 at peak hardness ($Hv \approx 485$) of $960\ \mathrm{MNm}^{-2}$ [3] leads to a relationship of the type $Hv \approx \sigma_y/2$. The calculated increment in flow stress of $400\ \mathrm{MNm}^{-2}$ would therefore correspond to an increment in hardness of $\Delta Hv \approx 200$. This value is in good agreement with the observed value of $\Delta Hv \approx 160$ between maximum and minimum hardness, Fig. 2a. A discrepancy would be expected since the order-hardening contribution should be greater after ageing at the higher temperature due to the larger volume fraction of γ' cuboids (0.3 compared with 0.21) [24], and also the lower total fraction at the higher temperature results in a larger contribution to solution hardening of the matrix (see below). Nevertheless, the maximum strength of IN-738 is mainly attributable to the high volume fraction of γ' spheroids after ageing at 1100 K. The decrease in hardness below this temperature is readily accounted for by incomplete precipitation of γ' spheroids.

Samples sequentially aged for 16 h at 1100 K followed by 16 h at 1315 K showed a hardness decrease from the maximum value of $Hv \approx 485$ to the minimum value of $Hv \approx 325$. However, reversing this heat treatment sequence resulted in a hardness of only $Hv \approx 380$. This further indicates the importance of the form and distribution of the γ' precipitates. The latter heat treatment sequence results in large ($\sim 0.6\ \mu\mathrm{m}$) γ' cuboids

which account for 0.30 of the total weight, so that subsequent ageing at 1100 K requires only a fraction of 0.15 γ' spheroids to precipate to achieve equilibrium. The former sequence results in a large fraction, 0.24, of γ' spheroids at 1100 K, which on further ageing at 1315 K either go into solution or contribute to the accelerated coarsening of the γ' cuboids [25].

From the minimum value of $Hv \approx 325$, the hardness increases to $Hv \approx 440$ as the isochronal ageing temperature is raised from 1315 to 1467 K, Fig. 2a. Over this temperature range the fraction of γ' precipitate, Fig. 2c, decreases from 0.3 to zero at the solvus temperature (1442 K). Such a decrease is dictated by the exact form of the equilibrium phase diagram. There is also a corresponding decrease in the fraction of MC carbide from 0.015 to 0.0095. Bieber and Mihalisin [3] suggest that the composition for γ' in IN-738 is:

$$(Ni_{0.922}, Co_{0.058}, Cr_{0.017}, Mo_{0.002}, W_{0.002})_3$$

$$(Al_{0.518}, Ti_{0.352}, Ta_{0.046}, Nb_{0.041}, W_{0.019}, Cr_{0.027})$$

whilst that for the MC carbides is:

$$(Ti_{0.50}, Ta_{0.20}, Nb_{0.20}, W_{0.04},$$

$$Mo_{0.03}, Cr_{0.02}, Zr_{0.01})C.$$

From the phase analyses of complex superalloys by Mihalisin and Pasquine [26], Kiege and Baris [7] and Loomis [27], Decker [12] lists the elements which contribute to solid solution hardening of γ phase as cobalt, iron, chromium, molybdenum, tungsten, vanadium, titanium and aluminium. Dissolution of γ' (and to a lesser extent carbides) above 1315 K will release all of these elements apart from iron and vanadium (not present) into the matrix. As reported previously [12], solid solution hardening can be related to atomic diameter mismatch together with an additional contribution from electron vacancy number. At least part of this contribution arises from a lowering of stacking fault energy by the alloying elements which tends to suppress cross-slip in the matrix. Of the present elements which contribute to solid solution hardening, aluminium would be the most effective [12].

5. Conclusions

(1) The solvus temperature for γ' precipitation in the superalloy IN-738 is 1442 ± 3 K. However, at this temperature dissolution of the carbides is incomplete. The recommended solution treatment temperature for IN-738 of 1393 K results in a significant fraction (0.2) of γ' precipitate being retained

(2) The hardness of isochronally aged IN-738 varies significantly over the temperature range 773 to 1467 K. Such hardness changes are related to the volume fraction, size and distribution of the γ' precipitates.

(3) Two forms of γ' precipitate are observed: spheroids of the order 0.1 μm diameter and degenerate cuboids of the order 0.5 μm mean diagonal.

(4) Over the temperature range 973 to 1473 K only one type of carbide, MC, is present and no borides.

(5) The major contribution to the peak hardness, at ~ 1100 K, is the large volume fraction of γ' spheroids.

(6) The rapid decrease in hardness after ageing between 1100 and 1315 K arises as a consequence of the decrease in the volume fraction of the γ' spheroids and an accompanying increase in their size.

(7) The measured hardness increase over the temperature range 1315 to 1467 K arises as a result of the dissolution of the coarse γ' degenerate cuboids which brings about a redistribution of solid solution hardening elements, particularly aluminium.

Acknowledgements

The assistance of Mr. M. B. Alloway is gratefully acknowledged. This paper is published with the permission of the Director-General, Central Electricity Generating Board, South Eastern Region.

References

1. P. R. SAHM, "High Temperature Materials in Gas Turbines", edited by P. R. Sahm and M. O. Speidel (Elsevier, New York, 1974) p. 73.
2. R. SIMMONS, *Gas Turbine World* **11** (1975) 28.
3. C. G. BIEBER, and J. R. MIHALISIN, 2nd International Conference on the Strength of Metals and Alloys, Asilomar, ASM Vol. IV, p. 1031.
4. R. W. FAWLEY, "The Superalloys", edited by C. T. Sims and W. C. Hagel, (Interscience, New York, 1972) p.17.
5. W. C. HAGEL and H. J. BEATTIE, *Iron and Steel Institute Special Report* **64** (1964) 98.
6. M. TAGAYA and I. TAMURA, *Nippon Kinzuku Gakki Sci.* **15** (1951) 144.
7. O. H. KRIEGE and J. M. BARIS, *Trans ASM* **62** (1969) 195.

8. E. H. VAN DER MOLEN, J. M. OBLAK and O. H. KRIEGE, *Met. Trans.* **2** (1971) 1627.
9. M. A. P. DEWEY and T. G. LEWIS, *J. Sci. Instrum.* **40** (1961) 385.
10. E. E. UNDERWOOD, "Quantitative Microscopy", edited by R. T. de Hoff and F. N. RHINES, (McGraw–Hill, New York, 1968) p.149.
11. H. E. COLLINS, *Met, Trans.* **5** (1974) 189.
12. R. F. DECKER and C. T. SIMS, "The Superalloys", edited by C. T. Sims and W. C. Hagel, (Interscience, 1972) p. 73.
13. R. F. DECKER, "Steel Strengthening Mechanisms", (Climax Molybdenum, Zurich, 1969) p. 147.
14. W. J. BOESCH and H. B. CANADA, *J. Met.* **4** (1968) 46.
15. J. M. OBLAK and B. H. KEAR, "Electron Microscopy and Structure of Materials", edited by G. Thomas (University of California Press, 1971) p. 566.
16. J. M. OBLAK, D. F. PAULONIS and D. S. DUVAL, *Met. Trans.* 5 (1974) 143.
17. A. J. ARDELL, *Phil. Mag.* **16** (1967)147.
18. H. BROOKS, "Interfaces", (ASM, Cleveland Ohio, 1952) p. 20.
19. N. S. STOLOFF, "The Superalloys", edited by C. T. Sims and W. C. Hagel, (Interscience, 1972) p.79.
20. E. OROWAN, "Symposium of Internal Stresses in Metals and Alloys", (Institute of Metals, London, 1948) p. 47.
21. A. KELLY and R. B. NICHOLSON, *Prog. Mater. Sci.* **10** (1963) 151.
22. L. M. BROWN and R. K. HAM, "Strengthening Mechanisms in Crystals", edited by A. Kelly and R. B. Nicholson, (Elsevier, New York, 1971) p.9.
23. D. J. ABSON, O. KOŠIK, J. L. UVIRA and J. J. JONAS, "The Science of Hardness Testing and its Research Applications", edited by J. H. Westbrook and H. Conrad (ASM, Cleveland, Ohio, 1971) p. 91.
24. H. GLEITER and E. HORNBOGEN, *Mater. Sci. Eng.* **2** (1968) 285.
25. J. J. WEINS, Ph.D. Thesis, Massachusetts Institute of Technology, 1970.
26. J. R. MIHALISIN and D. L. PASQUINE, International Symposium on Structural Stability in Superalloys, Seven Springs, Pa. 1968, 7, p. 134.
27. W. T. LOOMIS, Ph.D. Thesis, University of Michigan, 1969.

Received 15 April and accepted 8 July 1977.